Soft sweeps are the dominant mode of adaptation in the human genome

Daniel R. Schrider[*, †, 1] and Andrew D. Kern[*, †]

[*]Department of Genetics, Rutgers University, Piscataway, NJ, 08854, USA

[†]Human Genetics Institute of New Jersey, Rutgers University, Piscataway, NJ, 08554, USA

[1]Corresponding author: Department of Genetics, Rutgers University, 604 Allison Rd., Piscataway, NJ 08854. E-mail: dan.schrider@rutgers.edu

Keywords: adaptation, selective sweeps, soft sweeps, machine learning, population genomics

Running title: Adaptation via soft sweeps is prevalent in humans

ABSTRACT

The degree to which adaptation in recent human evolution shapes genetic variation remains controversial. This is in part due to the limited evidence in humans for classic "hard selective sweeps," wherein a novel beneficial mutation rapidly sweeps through a population to fixation. However, positive selection may often proceed via "soft sweeps" acting on mutations already present within a population. Here we examine recent positive selection across six human populations using a powerful machine learning approach that is sensitive to both hard and soft sweeps. We found evidence that soft sweeps are widespread and account for the vast majority of recent human adaptation. Surprisingly, our results also suggest that linked positive selection affects patterns of variation across much of the genome, and may increase the frequencies of deleterious mutations. Our results also reveal insights into the role of sexual selection, cancer risk, and central nervous system development in recent human evolution.

INTRODUCTION

Spurred by the ongoing revolution in DNA sequencing capacity, human population genetic datasets have grown exponentially in size over the past five years (Auton et al. 2015; UK10K Consortium 2015). Such growth enables insight into the evolutionary histories of human populations with hitherto unrivaled precision. A central question in the study of human evolution is the extent to which adaptation has driven recent evolution and affected patterns of genetic diversity (Akey 2009). This can be addressed by scanning genomic data for evidence of selective sweeps, wherein a beneficial mutation is favored by natural selection and therefore rapidly increases in frequency within a population. Such selective sweeps leave a characteristic footprint in variation; they create a valley of diversity around the selected site (Maynard Smith and Haigh

36 1974; Kaplan et al. 1989; Stephan et al. 1992), a deficit of both low- and high-frequency derived
37 alleles at linked sites (Fay and Wu 2000), and an increase in linkage disequilibrium in flanking
38 regions (Kim and Nielsen 2004). Thus there are multiple population genetic signals to exploit.
39 Accordingly numerous theoretical and methodological advances (Kaplan et al. 1989; Stephan et
40 al. 1992; Fu 1997; Kim and Stephan 2002; Nielsen et al. 2005b; Voight et al. 2006) in the study
41 of selective sweeps have given researchers the ability to uncover the genetic basis of adaptation
42 on a genome-wide scale.

43 There are two complimentary approaches to studying the impact of adaptive evolution on
44 genetic variation. The first approach aims to infer genome-wide rates of adaptive evolution by
45 estimating the mean effects of selective sweeps across the genome (Wiehe and Stephan 1993;
46 Kern et al. 2002; Andolfatto 2007; Jensen et al. 2008; Hernandez et al. 2011; Sattath et al. 2011).
47 Such approaches may estimate the rates of sweeps or their effects with respect to the genomic
48 background, but do not focus on the targets of sweeps themselves. An alternative approach is to
49 focus on finding individual selective sweeps throughout the genome, and in so doing characterize
50 specific cases of adaptation with hopes of gaining general insight into the adaptive process
51 (Sabeti et al. 2002; Voight et al. 2006; Williamson et al. 2007). The search for selective sweeps
52 has shed light into the recent evolutionary histories of natural populations, and has shown a
53 pervasive impact of adaptive evolution on polymorphism in some species such as *Drosophila*
54 *melanogaster* (Begun et al. 2007; Macpherson et al. 2007; Langley et al. 2012; Lee et al. 2013;
55 Garud et al. 2015). In humans, the picture remains less clear: while scans for selective sweeps
56 have discovered numerous compelling candidates for strong positive selection (e.g. Ruwende et
57 al. 1995; Stephens et al. 1998; Tishkoff et al. 2007; Bryk et al. 2008; Huerta-Sánchez et al.
58 2014), some recent studies have suggested that the impact of adaptation on patterns of variation

59 genome-wide is quite limited (Hernandez et al. 2011; Lohmueller et al. 2011). Conversely, Enard
60 et al. (2014) argue that the genome-wide reduction in diversity around substitutions is driven in
61 part by positive selection.

62 One possible explanation for the difficulty in characterizing the contributions of adaptive
63 and non-adaptive forces in human populations is that genetic hitchhiking effects may be muted
64 by human demographic history. Many human populations appear to have experienced
65 bottlenecks and/or recent growth (Marth et al. 2004; Fagundes et al. 2007; Gravel et al. 2011;
66 Auton et al. 2015), which cause much of the genome to resemble selective sweeps (Nielsen et al.
67 2005b). Moreover, positive selection has historically been modeled as the process of a *de novo*
68 beneficial mutation rapidly sweeping to fixation, a process now referred to as a hard sweep.
69 However selection may act on previously segregating neutral or weakly deleterious variants (Orr
70 and Betancourt 2001; Innan and Kim 2004). Selection on standing variation will produce
71 qualitatively different skews in linkage disequilibrium and allele frequencies, along with a
72 shallower valley in diversity (Hermisson and Pennings 2005; Przeworski et al. 2005; Berg and
73 Coop 2015; Schrider et al. 2015)—such an event is thus referred to as a soft sweep. If selection
74 typically proceeds through soft sweeps, as may be the case in Drosophila (Garud et al. 2015),
75 then many sweeps may have been missed by previous scans that were designed to detect
76 signatures produced under a hard sweep model.

77 We sought to address the controversy over the impact of adaptation on human genomic
78 variation by conducting a genome-wide scan for both hard and soft selective sweeps across
79 human populations. We previously developed S/HIC (Soft/Hard Inference through
80 Classification), a machine learning method capable of detecting completed sweeps and inferring
81 their mode of selection with unparalleled accuracy and robustness to non-equilibrium

82 demography (Schrider and Kern 2016). Here we apply S/HIC to uncover hard and soft sweeps in
83 six population samples from the 1000 Genomes Project (Auton et al. 2015), thereby performing
84 the most comprehensive investigation of completed selective sweeps in humans to date.
85 Surprisingly, our results suggest that patterns of polymorphism across much of the human
86 genome may be affected by linked positive selection—primarily soft sweeps. Moreover, we find
87 evidence that the mode of selection differs substantially across populations, with non-African
88 populations adapting via hard sweeps to a much greater extent than African populations. Finally,
89 we investigate the biological targets of selection in recent human evolution, with particular
90 processes such as immunity, cancer, and sexual reproduction playing outsized roles.
91

92 **RESULTS**

93 We set out to detect completed hard and soft selective sweeps in six populations from Phase 3 of
94 the 1000 Genomes Project: two West-African populations (YRI and GWD from Yoruba and The
95 Gambia, respectively), one East-African population (LWK from Kenya), one European
96 population (CEU, from Utah, USA), one East Asian population (JPT from Japan), and one from
97 the Americas (PEL from Peru). For each population we trained and applied a S/HIC classifier to
98 identify hard and soft selective sweeps across the genome (Methods), distinguishing them from
99 neutrally evolving regions as well as those linked to sweeps (Schrider and Kern 2016). Briefly,
100 S/HIC is a machine learning method that leverages spatial patterns of a variety of statistics across
101 a large genomic window in order to infer the mode of evolution at the center of the window. We
102 previously showed that S/HIC is exceptionally robust to the confounding effect of linked
103 selection (e.g. the "soft shoulder" effect where regions linked to hard sweeps resemble soft
104 sweeps; Schrider et al. 2015), as well as non-equilibrium demographic histories, making it well

105 suited for a survey of positive selection in humans. We also assessed the accuracy of our
106 classifiers on simulated test data with the same demographic history used to generate training
107 data, finding that S/HIC achieved good power for each demographic history, with somewhat
108 higher accuracy for histories inferred from the African than non-African populations
109 (supplementary fig. S1).

110 We also performed forward simulations under the GWD and JPT models (Methods) in
111 order to assess whether purifying selection and its effect on variation at linked unselected sites
112 (i.e. background selection Charlesworth et al. 1993) could result in false sweep calls. The results
113 of these simulations suggest that S/HIC's false positive rate is essentially unaffected by these
114 forces (supplementary fig. S1). Note that we exposed each classifier to a wide range of mutation
115 and recombination rates (see Methods) during training (and testing) in order to improve (and
116 assess) our robustness to variation in these rates across the genome. We also examined values of
117 Garud et al.'s (2015) H_{12} and H_2/H_1 within windows classified by S/HIC as hard, soft, or neutral,
118 noting that as expected, H_{12} is higher in sweeps than neutral regions, while H_2/H_1 is higher for
119 soft sweeps than hard sweeps (supplementary fig. S2). Below, we begin with a brief overview of
120 the broad patterns of adaptation we observe across populations, before discussing genomic
121 features and biological pathways with a strong enrichment of selective sweeps, as well as
122 compelling novel candidates for recently completed selective sweeps.

123

124 **The majority of sweeps in humans resemble selection on standing variation**

125 We found a total of 1,927 distinct selective sweeps merged across all six populations (Methods).
126 190 (9.9%) of these are present in all populations, 59 (3.1%) are shared among the African
127 populations, 71 (3.7%) are shared among the non-African populations, and 701 (36.4%) are

128 population-specific (supplementary table S1). The remaining 906 (47.0%) sweeps were present
129 in more than one population but do not fit into any of the categories above. We observe that
130 across populations, the vast majority (1,776, or 92.2%) of sweeps were classified as soft, and
131 note that this trend does not change qualitatively as we impose increasingly strict posterior
132 probability thresholds before assigning a class label to a given window (supplementary table S2;
133 Methods). These events may represent soft sweeps on standing genetic variants that our classifier
134 was trained to detect, but we note that a similar signature can be created by a soft sweep resulting
135 from recurrent origination of the adaptive allele(s), or by a *de novo* mutation that has been placed
136 onto multiple haplotypes by allelic gene conversion events (see Discussion).

137 Although hard sweeps appear to be quite rare globally, the fraction of hard sweeps is
138 significantly higher in non-African than African populations (table 1). For example, when
139 comparing PEL to GWD, we observe a significantly higher fraction of hard sweeps in PEL
140 (4.7% versus 1.6%; p=0.05). For each other African vs. non-African comparison we see an even
141 greater (and more significant) disparity. Further, we observe a suggestive correlation between the
142 fraction of sweeps in a population that were classified as soft and the harmonic mean of its
143 population size within the last 4N generations (Pearson's ρ=-0.96; Methods). Though taken at
144 face value this correlation appears to be highly significant, we note that due to the six
145 populations' shared evolutionary history a statistical test of this correlation would be invalid.

146 Comparing our results to those of previous scans we find that 519 of S/HIC's sweep calls
147 (26.9%) have previously been identified according to dbPSHP, a database of candidate regions
148 for recent positive selection across human populations (Li et al. 2013). This accounts for 10.9%
149 of the loci in the dbPSHP set (ignoring regions not classified by S/HIC). The remaining 1,408
150 sweeps called by S/HIC (73.1% of calls) represent potentially novel selective sweeps. There are

151 several possible explanations for the modest overlap between our set of sweep candidates and
152 those in dbPSHP. First, the sweep candidates in dbPSHP have been identified by a variety of
153 methods, some of which are designed to detect selective scenarios other than completed sweeps
154 (e.g. partial sweeps, spatially varying selection). Second, when comparing results from methods
155 designed to detect the same type of sweeps, the intersection between studies is often fairly small
156 (Akey 2009). Although most scans undoubtedly recover a large number of true selective sweeps,
157 different methods may produce different false positives and false negatives, resulting in
158 imperfect concordance between scans.
159

160 **Selective sweeps preferentially target genes involved in cancer and viral infection**

161 Examining the locations of selective sweeps across the genome, we find that regions classified as
162 selective sweeps are significantly overrepresented for both coding sequence and untranslated
163 regions (q<0.05 in several populations for hard sweeps, and each population for putative soft
164 sweeps; fig. 1A, B; supplementary table S3), relative to data sets with permuted classifications
165 (see Methods). Enrichment for transcription factor binding sites was less pronounced, and only
166 significant in soft sweeps for the three African populations along with PEL. The most striking
167 result we observed was a dramatic enrichment of sweep windows for mutations in the COSMIC
168 data set of somatic mutations that have been observed in cancer cells (Forbes et al. 2015) and
169 may therefore play a role in tumor suppression/progression. Averaged across populations, the
170 number of COSMIC mutations found in soft sweeps represents a 3.7-fold increase relative to that
171 observed in permuted data sets; this enrichment was significant in each population, and peaked at
172 4.5-fold in PEL. For hard sweeps, this enrichment was 12-fold on average, reaching as high as
173 21-fold in CEU, though this was the only population for which the enrichment was statistically

174 significant. We also observed a sizeable overrepresentation of genes encoding virus-interacting
175 proteins (VIPs) curated by (Enard et al. 2016) in soft sweeps, with a 1.9-fold increase relative to
176 permuted sets (averaged across populations). VIPs show a similar magnitude of enrichment in
177 hard sweeps for some populations, but does not achieve significance at $q<0.05$.
178

179 **Selective sweeps increase linked deleterious variation**

180 Because S/HIC not only detects selective sweeps, but also attempts to identify regions of the
181 genome that appear to be linked to recent sweeps, our classifications allow us to examine the
182 effect of linked selection in a principled way. We found that while a minority of genomic
183 windows were classified as selective sweeps (7.6% on average across all populations), a large
184 fraction of windows were classified as linked to a completed selected sweep, either hard or soft
185 (56.4% on average). These estimates range from 41.5% in JPT to 74.0% in GWD (fig. 2).

186 We also asked whether selective sweeps have a detectable impact on linked deleterious
187 variation. As beneficial alleles increase in frequency in a population, they may carry along with
188 them linked deleterious polymorphisms as hitchhikers, potentially increasing the frequency of
189 deleterious variants over what would be expected given mutation-selection-drift equilibrium
190 (Birky and Walsh 1988; Hartfield and Otto 2011). To this end we asked whether relatively
191 common candidate deleterious mutations were enriched in regions classified as either hard-
192 linked or soft-linked. Indeed, we observed a fairly subtle but significant overrepresentation of
193 SNPs with derived allele frequencies of at least 0.01 but predicted to be damaging by SIFT
194 (Kumar et al. 2009) in both the hard-linked (mean enrichment across populations: 1.3-fold) and
195 soft-linked (mean enrichment: 1.1-fold) classes for most populations (fig. 1C, D; supplementary
196 table S3). We find a similar enrichment in these sweep-linked classes of common SNPs in

197 regions inferred to be conserved across primates according to phastCons (Siepel et al. 2005).
198 Phenotype-associated variants from the GWAS catalogue (Welter et al. 2014) were also
199 significantly overrepresented sweep-linked regions in several populations (Fig 1C, D).
200

201 **Sexual reproduction, the central nervous system, and immunity are targets of recent**
202 **sweeps**

203 In order to determine if positive selection preferentially acts on particular organismal functions,
204 we asked which Gene Ontology (GO) terms were enriched in our sweep calls relative to the
205 permuted data (Methods). In soft sweeps, we found a sizeable and significant enrichment
206 (q<0.05) of terms related to sperm development, structure, and function. For example,
207 "spermatogenesis" (4.4-fold enrichment averaged across populations), and "sperm-egg
208 recognition" (3.9-fold enrichment on average) were enriched in soft sweeps in several
209 populations. We also observed an overrepresentation of genes involved in the "glutamate
210 receptor signaling pathway" in our soft sweep sets for each population (4-fold mean enrichment).
211 Glutamate receptors are the primary excitatory neurotransmitter in the central nervous system,
212 and important for both proper brain development and function (Luján et al. 2005). Indeed, soft
213 sweeps are enriched for "central nervous system development" in multiple populations (1.6-fold
214 mean enrichment). Numerous GO terms related to immune response, especially adaptive
215 immunity, as well as KEGG pathways related to immunity and cancer progression/tumor
216 suppression were also significantly enriched among soft sweeps (see supplementary table S4 for
217 full list).
218

219 **Positive selection on interacting gene pairs**

220 We examined three types of gene interaction networks: protein-protein interactions (PPIs),
221 transcription factor-target gene interactions, and genetic interactions where one gene modifies
222 the effect of another (Methods). Interestingly, we observed a dramatic enrichment of sweeps in
223 genes that encode proteins that physically interact with one another (fig. 3A–B): if a gene
224 overlapped a window classified as a soft sweep, genes that interact with this gene were on
225 average 3.3 times more likely to overlap a putative soft sweep than expected by chance
226 (p<0.0001 for each population; fig. 3B). Despite the smaller number of candidate regions, we
227 found a significant enrichment for PPIs in hard sweeps, though this was only significant in for
228 non-African populations (4.0-fold enrichment averaged across populations; p<0.05 in CEU, JPT,
229 YRI; fig. 3A). For transcription factor-target interactions, we observe no overrepresentation of
230 soft sweeps, but a significant enrichment of hard sweeps in non-African populations (p<0.05 for
231 each; 8.5-fold enrichment on average; fig. 3C–D). There were no populations exhibiting an
232 overrepresentation of pairs of genes with genetic interactions and experiencing sweeps of either
233 type (fig. 3E–F).
234

235 **Examples of novel selective sweep candidates**

236 In this section we describe several sweep candidates that exemplify the set of sweeps, and
237 functions of putative targets of selection, that we were able to detect. As discussed above, our
238 sets of sweeps were highly enriched for glutamate receptor-encoding genes. In supplementary
239 fig. S3, we show a sweep candidate region on chromosome 4 that encompasses the glutamate
240 receptor gene *GRIA2*. This sweep was previously detected in non-African populations by
241 Pickrell et al. (2009), who did not find any evidence of selection in Africa. However, S/HIC
242 infers that this region has experienced a soft sweep that is found in GWD and YRI, as well as the

243 non-African populations. Consistent with this, Europeans, Asians, and African populations show
244 a reduction in π, a trough in Tajima's *D* (Tajima 1989), and a peak in Nielsen et al.'s
245 SweepFinder composite likelihood ratio (CLR) test statistic, which captures regions that appear
246 to be at the epicenter of the spatial skew in the SFS expected around sweeps (Nielsen et al.
247 2005b). Intriguingly, *GRIA2* interacts with the *GRID2* glutamate receptor gene (Kohda et al.
248 2003), which itself is classified as a soft sweep in CEU, LWK, PEL, and GWD. The remaining
249 glutamate receptors overlapping identified sweeps are *GRIA4*, *GRID1*, *GRIK1*, *GRIK3*, *GRM2*,
250 and *GRM7*. Of these genes, *GRIA4* and *GRID2* were shown by Liu et al. (2012) to have evolved
251 a human-specific developmental expression profile.

252 Fig. 4 shows a region on chromosome 9 that exhibits strong evidence of a previously
253 undetected hard sweep in each of our six populations. This region contains several members of
254 the spermatogenesis associated 31 gene family: *SPATA31B1*, *SPATA31D1*, *SPATA31D3*, and
255 *SPATA31D4*. Across populations this region shows dramatic valleys in π and Tajima's *D*, as well
256 as an elevated CLR near the center of the sweep window. These genes are highly testis-specific
257 according to data from the GTEx project (Lonsdale et al. 2013), and male mice are infertile when
258 lacking Spata31, another member of these gene family (Wu et al. 2015). fig. 4 also shows that
259 each of these genes overlaps a cluster of non-repetitive piRNAs (data from piRBase; Zhang et al.
260 2014). Also near this region is *DDX10P2*, which GENCODE annotates as a processed
261 pseudogene (Pei et al. 2012). *DDX10P2*, which is located at the center of the CLR peak for CEU,
262 is expressed with a high degree of testis-specificity according to GTEx data, similar to the
263 neighboring *SPATA31* genes. A BLAT search (Kent 2002) revealed that this putative
264 pseudogene exhibits 99.5% sequence identity to the orthologous sequence in chimpanzees. The

265 parent gene of *DDX10P2*, *DDX10*, is expressed in many tissues, but shows highest expression in
266 the testis.

267 On chromosome 11 we detected what appear to be several novel soft sweeps present in
268 and upstream of *CADM1* (cell adhesion molecule 1; fig. 5), one of which is present in each
269 population. This gene is essential for spermatogenesis in mice (Van Der Weyden et al. 2006),
270 and is also a tumor suppressor that is hypermethelated in various cancers (Kuramochi et al. 2001;
271 Allinen et al. 2002; Fukuhara et al. 2002), as it works with the adaptive immune system to
272 suppress metastasis (Faraji et al. 2012). *CADM1* is also active in the brain where it is involved in
273 synaptic adhesion and has been linked to autism (Zhiling et al. 2008; Fujita et al. 2010). *CADM1*
274 forms a complex with two other genes: the GABA receptor *GABBR2*, which has a soft sweep in
275 YRI, and *MUPP1*, which has a soft sweep found in each population; this complex appears to
276 localize to Purkinje cell dendrites (Fujita et al. 2012). Thus, this example encompasses many of
277 the functions that we find are highly enriched across our sweep sets: adaptation in multiple
278 interacting genes (one of which is a neurotransmitter), spermatogenesis, and tumor suppression
279 (via adaptive immunity).

280

281 **DISCUSSION**

282 Understanding the history of human adaptation at the genetic level is a central goal of population
283 genomics and human evolutionary biology. Accordingly, since the completion of the human
284 genome assembly (Lander et al. 2001) and subsequent proliferation of population genomic data,
285 numerous genome-wide scans for selection have been conducted using differing methodologies
286 (Sabeti et al. 2002; Voight et al. 2006; Sabeti et al. 2007; Pickrell et al. 2009; Field et al. 2016).
287 The majority of these studies searched primarily for partial selective sweeps—the signature of a

288 beneficial mutation currently sweeping through a population (see Williamson et al. 2007 for a
289 notable exception)—and rightly so, as these sweeps can reveal the targets of ongoing adaptation
290 in human populations. However, because the sojourn of an adaptive mutation to fixation should
291 be rapid (e.g. on the order of 400 generations, assuming N=10^4 and a moderately strong selection
292 coefficient of s = 0.05, and 4000 generations for s=0.005), the success of efforts to detect
293 ongoing selection implies the presence of a larger number of recently completed sweeps. We
294 have therefore focused on completed sweeps in order to complement previous studies and to
295 construct a more comprehensive catalogue of the loci underpinning recent human adaptation.
296 Using a powerful and robust machine learning method that we have recently introduced (S/HIC;
297 Schrider and Kern 2016) for finding completed selective sweeps, we performed a genome-wide
298 search for the targets of recent positive selection in six human populations. Furthermore, we
299 sought to determine the mode of positive selection, distinguishing between selection on *de novo*
300 mutations and on previously standing variation.
301
302 **Soft sweeps dominate human adaptation**
303 Perhaps our most consequential result is the finding that the majority of our candidate sweeps
304 resemble soft sweeps on standing variation. This result implies that adaptation in humans may
305 not be mutation-limited (Gillespie 1991; Karasov et al. 2010): rather than waiting for a novel
306 mutation to arise, human populations may often be able to respond via selection on previously
307 segregating polymorphisms, thereby more rapidly responding to novel environmental challenges.
308 This may be surprising given the apparently small effective population size and low nucleotide
309 diversity levels in humans. However, if the mutational target for the trait to be selected on is

310 fairly large, then the probability of a population harboring a mutation affecting that trait may be
311 appreciable.

312 While soft sweeps appear to be the dominant mode of selection globally, there is a
313 significant increase in the proportion of putative hard sweeps in non-African populations relative
314 to African populations. This is consistent with theoretical expectations, as larger populations
315 have more standing variation for selection to act on (Hermisson and Pennings 2005). Moreover,
316 the human migration out of Africa was associated with a severe population bottleneck (Marth et
317 al. 2004; Fagundes et al. 2007). Soft selective sweeps may be "hardened" by a reduction in
318 population size, which can result in the stochastic loss of some genetic backgrounds harboring
319 the adaptive allele so that only a single haplotype reaches fixation (Wilson et al. 2014). Thus,
320 though one might expect selection on segregating neutral or nearly neutral variation when a
321 population enters a new environment with novel selective pressures, if the migration event is
322 accompanied by a bottleneck then the population may experience a somewhat counterintuitive
323 increase in the proportion of hard sweeps. Moreover, the causal relationship between population
324 size and mode of adaptation may not be unidirectional. As Orr and Unckless (2014) have shown
325 in the context of evolutionary rescue, when faced with a changing environment, a population
326 which does not harbor standing variation that is beneficial may experience a more protracted
327 decline in size while it waits for an adaptive *de novo* mutation.

328 Our genome-wide results amplify results of earlier studies that by design have tried to
329 infer the mode of adaptation in a smaller number of targeted loci. For instance Peter *et al.* (Peter
330 et al. 2012) attempted to infer the mode of adaptation among 7 loci previously identified to be
331 under selection in human populations. They report that half of the loci that they could
332 confidently classify supported selection on standing variation. In *Drosophila melanogaster,*

333 when looking among strong outliers of haplotype homozgosity, Garud *et al.* (2015) found that
334 patterns of variation in those regions were consistent with recent soft selective sweeps. Our
335 finding, that the vast majority of sweeps in human populations are soft sweeps, thus underscores
336 the ubiquity of selection from standing variation in natural populations. Indeed it seems plausible
337 that adaptation from standing variation might be the rule, rather than the exception.

338 There are two caveats affecting our ability to discriminate between selection on standing
339 variation and on *de novo* mutations. First, while we have trained our classifier to detect soft
340 sweeps on previously segregating mutations, soft sweeps may also occur via recurrent mutation
341 to the adaptive allele (Pennings and Hermisson 2006b, a). Though there are some qualitative
342 differences between these two models of soft sweeps (Berg and Coop 2015; Schrider et al.
343 2015), these are fairly subtle in comparison to the differences between the other models we
344 consider. Thus, our classifiers may have sensitivity to both types of sweeps. If this is so, then
345 some of the soft sweeps that we detect may result from recurrent mutation. Additionally, gene
346 conversion during a sweep can transfer the adaptive mutation on to new genetic backgrounds
347 (Jones and Wakeley 2008), thereby "softening" the sweep (Schrider et al. 2015). This implies
348 that selection on a single *de novo* mutation could sometimes appear to be a soft sweep in our
349 classification. In any case, our finding that most sweeps in humans do not appear to be hard
350 sweeps underscores the importance of using methods that are sensitive to soft sweeps.

351

352 **Extensive impact of linked positive selection**

353 Our analysis demonstrates that the impact of linked positive selection on genetic variation is
354 considerable, with roughly half of the genome classified by S/HIC as being influenced by a
355 nearby sweep. This result has important implications for efforts to infer demographic histories

356 from patterns of genetic polymorphism, as most inference methods hinge on the assumption of
357 neutrality. Indeed, we have recently shown that linked positive selection has the potential to
358 severely confound demographic inferences (Schrider et al. 2016). Similarly, Ewing and Jensen
359 (2016) have found that background selection (Charlesworth et al. 1993) can also bias
360 demographic estimates. One strategy is to use only those polymorphisms that are distant from
361 genes and conserved noncoding elements to mitigate these effects (Gazave et al. 2014). One
362 could further supplement such an approach by using S/HIC to directly ask which intergenic
363 regions are unaffected by hitchhiking in order to further diminish the bias introduced by linked
364 selection. We note that the putatively neutrally evolving regions found in this study can be
365 obtained from our raw classification output (available at https://github.com/kern-
366 lab/shIC/tree/master/humanScanResults).

367 If linked positive selection affects much of the genome, then that implies that the
368 frequencies of many neutral or weakly deleterious mutations may be altered by genetic draft
369 (Gillespie 2000). That is to say, deleterious mutations that happen to reside on chromosomes that
370 begin to sweep may be able to reach higher frequencies than expected from mutation-selection-
371 drift equilibrium. Consistent with this, we observe a slight but significant excess of potentially
372 deleterious polymorphisms in windows classified as linked to selective sweeps. Previously, Chun
373 and Fay (2011) found evidence that the ratio of deleterious to neutral polymorphisms is elevated
374 in sweep regions, concluding that hitchhiking carries linked deleterious variants to higher
375 frequencies. Our finding that SNPs from the GWAS catalogue are also enriched regions linked to
376 selective sweeps lends further support to this hypothesis. Indeed, several compelling examples of
377 hitchhiking mutations known or suspected of causing disease have been described in the
378 literature (Helgason et al. 2007; Chun and Fay 2011; Huff et al. 2012). Moreover it seems that

379 the phenomenon of deleterious alleles hitchhiking along with strongly beneficial alleles is not
380 restricted to humans: a recent study also uncovered evidence that selection during domestication
381 increased the frequency of deleterious polymorphisms in dogs (Marsden et al. 2016).
382
383 **Targets of recent human selective sweeps**
384 Our catalogue of sweep candidates allowed us to characterize the biological functions that are
385 overrepresented in sweeps. Notably, we found a strong excess of spermatogenesis genes within
386 sweep regions, a phenomenon previously observed by Voight et al. (2006). This signature may
387 be a result of sexual selection, sexual conflict, and/or sperm competition (Swanson and Vacquier
388 2002). We also observed a significant enrichment of cancer-related genes among our sweep
389 candidates. Nielsen et al. (2005a) found a similar enrichment of candidate genes under selection
390 related to cancer when examining protein divergence between humans and chimpanzees. These
391 authors found that some of these genes are also involved in spermatogenesis (much like our
392 *CADM1* example), and concluded that genomic conflict between tumor suppression and the
393 advantage of avoiding apoptosis during spermatogenesis may explain the selection on cancer
394 genes. An alternative (and non-mutually exclusive) explanation is that the increase in longevity
395 along the human lineage has created an immense selective pressure to reduce the rate of cancer
396 progression by orders of magnitude (Nunney and Muir 2015).
397 We also observed a significant excess of glutamate receptor genes targeted by sweeps,
398 suggesting that these loci may underlie some of the dramatic neurological changes that have
399 occurred along the human lineage. Consistent with this, we previously found evidence
400 suggesting some of these glutamate receptor genes (along with other neurotransmitters) may
401 have recently gained novel regulatory elements in humans (Schrider and Kern 2015; Meyer et al.

402 2017). The most striking examples of glutamate receptors experiencing sweeps are *GRIA2* and
403 *GRID2*, which show strong signatures of selection in multiple populations and physically interact
404 with one another. The action of positive selection on multiple members of the protein complex
405 appears to be a general phenomenon (fig. 3). For a more in-depth examination of positive
406 selection in the PPI network, see Qian et al. (2015), who found that genes in candidate regions
407 for positive selection were more likely to lie close together in the PPI network.
408

409 **Conclusions**

410 Our investigation has revealed several valuable insights into the adaptive process in human
411 populations. The success of our approach exemplifies the potential of machine learning methods
412 to elucidate the adaptive process in humans and other species (Fan et al. 2016). To date several
413 machine learning methods have been devised to detect selective sweeps (Pavlidis et al. 2010; Lin
414 et al. 2011; Ronen et al. 2013; Pybus et al. 2015; Sheehan and Song 2016), and they tend to
415 substantially outperform more traditional approaches (see Schrider and Kern 2016). We suspect
416 that machine learning could be used to make important inroads in answering a variety of
417 evolutionary questions.

418 Finally, Hernandez et al. (2011) argued that hard selective sweeps might be rare in human
419 populations, and instead suggested that the majority of adaptation might be a consequence of
420 selection on standing variation or selection on polygenic traits. We here find direct evidence that
421 indeed this is the case—the vast bulk of human adaptation is occurring as a consequence of soft
422 sweeps. Our observation thus reconciles Hernandez et al.'s findings with those of Enard et al.,
423 who conclude that the reduction in diversity around amino acid substitutions is caused by
424 widespread selective sweeps (Enard et al. 2014). Moreover, while our scan leveraged a method

425 that performs very well in detecting both hard and soft sweeps, it was not trained to detect cases
426 of polygenic selection (e.g. Berg and Coop 2014). It is fair to assume that a large majority of
427 phenotypes are determined by multiple loci, thus polygenic selection should be expected to be
428 common. If that were the case, then it could very well be that an even larger portion of genetic
429 variation is influenced by natural selection and its linked effects throughout the genome.
430

431 **METHODS**

432 **Sequence and annotation data**

433 We downloaded phased genotype data from Phase 3 of the 1000 Genomes Project (Auton et al.
434 2015). This data set consists of 26 population samples from Africa, East Asia, South Asia,
435 Europe, and the Americas. We wished to include only populations where the influence of
436 admixture/migration on genetic variation appeared to be minimal, while still allowing us to
437 characterize selection across multiple continents. We therefore chose to scan the following
438 populations for selective sweeps: the GWD (Gambians in Western Divisions in The Gambia) and
439 YRI (Yoruba in Ibadan, Nigeria) populations from West Africa, LWK (Luhya in Webuye,
440 Kenya) from East Africa, JPT (Japanese in Tokyo, Japan) from Asia, CEU (Utah residents with
441 Northern and Western European Ancestry) from Europe, and PEL (Peruvians from Lima, Peru)
442 from the Americas. Examining Auton et al.'s results from running ADMIXTURE (Alexander et
443 al. 2009), we see that for most values of *K*, each of these populations appears to correspond
444 primarily to a single ancestral population rather than displaying multiple clusters of ancestry (see
445 Extended Data Figure 5 from Auton et al. 2015). One exception may be the PEL population, but
446 among the highly admixed American samples it appears to exhibit the smallest amount of
447 possible mixed ancestry (for most values of *K*), so we retained this population in order to have

448 some representation from the Americas. We opted not to examine any South Asian population,
449 as for each of these samples ADMIXTURE inferred evidence of ancestry from three or more
450 ancestral populations.

451 We downloaded numerous annotation data sets containing genomic features to test for
452 enrichment/depletion of selective sweeps and perform other downstream analyses. These
453 included GENCODE gene model release 19 (Harrow et al. 2012) including pseudogenes (Pei et
454 al. 2012), virus-interacting proteins from Enard et al. (2016), enhancers gained or along the
455 human lineage since diverging from Old World monkeys (Cotney et al. 2013), and SIFT's
456 (Kumar et al. 2009) predictions of damaging amino acid polymorphisms from dbNSFP version
457 3.2a (Liu et al. 2016). We obtained Gene Ontology (GO) annotations from ENSEMBL release
458 75 (Yates et al. 2016). We also downloaded coordinates of previously identified selective sweeps
459 from dbPSHP (Li et al. 2013).

460 We used the UCSC Table Browser (Karolchik et al. 2004) to obtain the following data
461 sets: phenotype-associated SNPs from the GWAS Catalog (accessed Apr 12, 2016; Welter et al.
462 2014), ClinVar pathogenic SNPs and indels ≤ 20 bp in length (Apr 26, 2016; Landrum et al.
463 2016), COSMIC somatic mutations in cancer (accessed Feb 25, 2014; Forbes et al. 2015),
464 phastCons elements conserved across primates (accessed Jun 2, 2013; Siepel et al. 2005),
465 ENCODE transcription factor binding sites version 3 (accessed Aug 25, 2013; Dunham et al.
466 2012), tables of genes and SNPs implicated in Mendelian phenotypes from OMIM (accessed
467 May 2, 2016; Amberger et al. 2015), and KEGG pathway annotations (accessed Apr 27, 2016;
468 Kanehisa et al. 2015). For each of these data sets we used GRCh37/hg19 coordinates.

469 In order to examine the prevalence of selective sweeps within interacting gene networks,
470 we downloaded physical and genetic interactions from BioGRID version 3.4.136 (Chatr-

471 Aryamontri et al. 2015). Our set of genetic interactions consisted of those annotated as "synthetic
472 genetic interaction defined by inequality," "suppressive genetic interaction defined by
473 inequality," or "additive genetic interaction defined by inequality." Physical interactions
474 included those annotated as "direct interaction," "association," or "physical association." We
475 extracted transcription factor-target interactions from ORegAnno (accessed Dec 22, 2015;
476 Griffith et al. 2008), retaining only interacting pairs where the ENSEMBL gene identifier were
477 provided for both genes in order to avoid ambiguity.
478
479 **Building classifiers to detect selective sweeps**
480 To detect sweeps we used S/HIC (https://github.com/kern-lab/shIC), a machine learning
481 approach we previously described and showed to be remarkably powerful and robust to non-
482 equilibrium demography (Schrider and Kern 2016). Briefly, the S/HIC machine learning
483 approach leverages spatial patterns (along a genome) of a variety of population genetic summary
484 statistics to classify genomic windows as being the target of a completed hard sweep (hard),
485 being closely linked to a hard sweep (hard-linked), a completed soft sweep (soft), linked to a soft
486 sweep (soft-linked), or evolving neutrally (neutral). While this classification approach allows
487 inference when considering a large number of features jointly, it necessitates training from a
488 large number of data instances known to belong to each class. Because the number of genomic
489 windows known to belong to each our five classes is limited, we must rely on simulation to
490 generate our training data. To this end we used the program discoal (Kern and Schrider 2016) to
491 simulate large chromosomal regions, subdivided into 11 sub-windows. Training examples for the
492 hard class experienced a hard sweep in the center of the central sub-window (i.e. the 6th
493 window), while examples for the hard-linked class experienced a hard sweep in the center of one

494 of the remaining sub-windows (selected randomly). Analogous simulations with soft sweeps
495 were generated for the soft and soft-linked classes, respectively. Finally, neutrally evolving
496 examples did not experience any selective sweep.

497 We sought to train a classifier for each population under a demographic model that offers
498 a better approximation to the population size history than the standard neutral model. For this we
499 used Auton et al.'s (2015) population histories inferred by PSMC (Li and Durbin 2011). The
500 1000 Genomes Project's PSMC output did not contain estimates of θ, the population mutation
501 rate parameter. Thus for each population we conducted a grid search by simulating genomic
502 windows with the appropriate sample size under each demographic model with varying values of
503 θ=4NuL (where L is the length of the locus, which we set to 100 kb); the grid of θ values raged
504 from 10 to 250, examining multiples of 10. For each value of θ, we compared the values of π
505 (Nei and Li 1979), $\hat{\theta}_w$ (Watterson 1975), $\hat{\theta}_H$ (Fay and Wu 2000), H_2/H_1 (Garud et al. 2015), and
506 Z_{nS} (Kelly 1997) from 1000 simulations to those from 1000 randomly selected genomic loci
507 (calculated as described below), calculating the mean of each statistic in the real and simulated
508 datasets. We chose as the final values of θ that for which the sum of the percent deviations of the
509 simulated from the observed means of each statistic was minimized. This estimate of θ allowed
510 us to calculate estimated population sizes and times scaled by the number generations for each
511 time point in the history inferred by PSMC. The harmonic mean of each population's size was
512 calculated by taking the estimated population size for each of the last 4N generations. We note
513 that these models may not accurately capture the demographic histories of the populations we
514 examined due to the confounding effects of positive (Schrider et al. 2016) and negative (Ewing
515 and Jensen 2016) selection. However, because of S/HIC's robustness to demographic
516 misspecification, we do not expect this to severely impact our analysis (Schrider and Kern 2016).

517 For each population we simulated a total of 2000 regions for each of our five classes. For
518 simulations involving sweeps, we drew the selection coefficient from $U(0.005, 0.1)$, the sweep
519 completion time from $U(0, 2000)$, the initial selected frequency for soft sweeps from $U(1/N, 0.2)$.
520 We drew values of θ uniformly from a range spanning exactly one order of magnitude, specified
521 so that the mean value of θ was equal to that estimated for the population as described above. We
522 drew recombination rates from an exponential distribution with mean 1×10^{-8}, truncated at triple
523 the mean due to memory constraints. The simulation program discoal requires some of these
524 parameters to be scaled by the present-day effective population size; we did this by taking the
525 mean value of θ and dividing by $4uL$, where u was set to 1.2×10^{-8} (Kong et al. 2012). The full
526 command lines we used to generate 1.1 Mb regions (to be subdivided into 11 windows each 100
527 kb in length) for each population are shown in supplementary table S5. We also simulated 1000
528 test examples for each population in the same manner as for the training data.

529 In order to address the potential for purifying and background selection to confound our
530 classifiers, we simulated additional test sets of 1000 genomic windows 1.1 Mb in length with
531 varying arrangements of selected sites. In order to mimic patters of purifying/background
532 selection expected in the human genome as closely as possible, for each of our 1000 replicates
533 we randomly selected a 1.1 Mb window from the human genome and asked which sites were
534 found within either a GENCODE exon (Harrow et al. 2012) or within a phastCons (Siepel et al.
535 2005) conserved element from the UCSC Genome Browser's 100-way vertebrate alignment
536 (Kent et al. 2002). Sites in the simulated chromosome corresponding to these functional elements
537 in the human genome were labeled as "selected" in the simulations. In "selected" regions, 25%
538 of all new mutations had no fitness effect, while the remaining 75% had a selection coefficient
539 drawn from a gamma distribution with mean of −0.0294 and a shape parameter of 0.184 (the

540 African model from Boyko et al. 2008). We limit fitness effects of new mutations to 75% in an
541 effort to mimic coding regions of the genome. We note that this percentage may not be accurate
542 for noncoding functional regions, though it is likely that some fraction of mutations in these
543 regions is effectively neutral. All mutations outside of the selected regions were fitness-neutral.
544 These simulations were performed for both our GWD and JPT demographic models using the
545 fwdpy11 (https://github.com/molpopgen/fwdpy11) forward population genetic simulator
546 (Thornton 2014), using the same mutation rates, recombination rates, and history of
547 instantaneous population size changes as used in our coalescent simulations described in
548 supplementary table S5. Feature vectors were then generated for each of these simulated test
549 examples in the same manner as for our coalescent simulations. We also tested each population's
550 classifier against test sets generated by discoal with different fixed values of θ (but otherwise
551 with the same parameterizations shown in supplementary table S5) in order to ensure that our
552 approach was robust to uncertainty in the estimate of this parameter (supplementary fig. S4).

553 Our feature vector for each simulated region examined the spatial patters (following
554 Schrider and Kern 2016) of each of the following statistics: π (Nei and Li 1979), $\hat{\theta}_w$ (Watterson
555 1975), $\hat{\theta}_H$ (Fay and Wu 2000), the number of distinct haplotypes, average haplotype
556 homozygosity, Garud et al.'s (2015) H_{12} and H_2/H_1 statistics, Z_{nS}, ω (Kim and Nielsen 2004), and
557 the maximum frequency of derived mutations (Li 2011). Before calculating these summary
558 statistics we masked a number of sites within each simulation by randomly selecting a 1.1 Mb
559 region from our empirical windows sampled throughout the genome and masking the same
560 regions in the simulated window as were masked in the genomic window (see below). Thus our
561 simulated windows exhibit the same distribution of regions of missing data as the windows to

562 which we applied our classifiers. We then used S/HIC to train extra-trees classifiers (Geurts et al.
563 2006), one for each population.
564
565 **Classifying genomic windows in each population**
566 Having trained our classifiers, we then applied them to genomic data from the corresponding
567 population. We inferred ancestral states of polymorphisms and masked inaccessible sites
568 (whether polymorphic or not) in the same manner as described previously (Schrider and Kern
569 2016). We then used S/HIC to classify the central 100 kb sub-window of 1.1 Mb windows across
570 the autosomes, while taking the stringent approach of omitting those for which any sub-window
571 was less than 25% accessible, before sliding 100 kb downstream to examine the next window.
572 We also removed windows where any of the three central sub-windows had a mean
573 recombination rate of zero (using data from Kong et al. 2010). Importantly, for each retained 1.1
574 Mb window, we recorded the locations of all sites deemed inaccessible for use in masking our
575 training data (see above). In total we classified 13,968 windows, accounting for 48.5% of the
576 assembled autosomes. For our classifications we simply took the class that S/HIC's classifier
577 inferred to be the most likely one, but we also used S/HIC's posterior class membership
578 probability estimates in order to experiment with different confidence thresholds (results shown
579 in supplementary table S2). For a given threshold, we required the sum of a windows' hard and
580 soft sweep posterior probabilities to be greater than or equal to the threshold before labeling the
581 window as a sweep; the mode of the sweep was that corresponding to the greater posterior
582 probability among the hard and soft sweep classes.
583 In order to count the number of distinct sweep candidates found within our set of
584 populations , we simply merged all 100 kb windows classified as a sweep of either type that were

located either at the exact same coordinates or adjacent to one another, repeating this until no more sweep regions could be merged. If all constituent windows were classified as soft, we counted the sweep as soft; otherwise we counted it as a hard sweep. We used a similar approach but examining classifications from only one population at a time in order to count the number of sweeps of each type in that population. If a gene found within a sweep window identified by S/HIC was not found in an entry of dbPSHP (Li et al. 2013), we referred to it as a novel sweep. Visualization of sweep candidates was performed using the UCSC Genome Browser (Kent et al. 2002) , along with custom tracks showing values of various population genetic summary statistics and selection scan scores for the CEU, YRI, and JPT populations from the Human Positive Selection Browser (Pybus et al. 2013). Our classification results are available at https://github.com/kern-lab/shIC/tree/master/humanScanResults.

Permutation tests for enrichment of annotation features in sweeps

To determine whether certain annotation features were enriched within any of our five classes, we carefully designed a permutation test to account for the subset of the genome that we examined with S/HIC, as well as the spatial correlation of S/HIC's classifications (i.e. adjacent windows are especially likely to receive the same classification). Briefly, the permutation algorithm begins by examining our classification results for a given population and keeping track of the length of runs of consecutive windows assigned to each class. The permutation algorithm then selects a chromosome, and begins at its first classified window (i.e. not removed by data filtering). A run length and associated class assignment is then randomly drawn without replacement. This process continues until the end of the chromosome, and then another chromosome is selected until the end of the final chromosome is reached, at which point the

608 permutation has been completed. We then repeated this permutation procedure 10,000 times for
609 each population. Note that this process preserves the run length distribution of our classifications
610 while permuting them across the set of genomic windows that had enough unmasked data to be
611 included in our scan.

612 After constructing our permuted data sets, we conducted one-sided enrichment tests by
613 counting the number of base pairs in the intersection between the S/HIC class of interest and the
614 annotation feature of interest, and comparing this number to its distribution among the permuted
615 data sets. The fraction of permuted data sets where this intersect was greater than or equal to that
616 observed for the real data is the *p*-value. Because we tested each of S/HIC's five classes for
617 enrichment of a fairly large number of genomic features (supplementary table S3), we corrected
618 for multiple testing using false discovery rate *q*-values following Storey (2002). When testing
619 GO terms and KEGG pathways for enrichment, we considered only the hard and soft sweep
620 classes, corrected for calculating *q*-values separately for each class.

621 We also asked whether the number of pairs of interacting genes both overlapping
622 windows classified as sweeps was greater than in our permuted data sets. To ensure that our
623 results were not inflated by the spatial clustering of interacting genes, we only counted
624 interacting pairs overlapping sweep windows if they were separated by at least 10 Mb or on
625 separate chromosomes. In addition, if we observed an interaction between two genes, *A* and *B*,
626 that each overlapped sweeps, and a third sweep candidate gene, *C*, was found, to avoid
627 redundancy we counted at most one interaction between *A* and *C* and *B* and *C*, even if *C* was
628 found interact with both other genes. As with GO and KEGG terms, we only searched the hard
629 and soft classes for enrichments before calculating one-sided q-values as described above.
630

ACKNOWLEDGMENTS

We thank Matthew Hahn, David Enard, and three anonymous reviewers for feedback on the manuscript. D.R.S. was supported in part by NIH award no. K99HG008696. A.D.K. was supported in part by NIH award no. R01GM078204.

REFERENCES

Akey JM. 2009. Constructing genomic maps of positive selection in humans: Where do we go from here? *Genome Res* 19: 711-722.

Alexander DH, Novembre J and Lange K. 2009. Fast model-based estimation of ancestry in unrelated individuals. *Genome Res* 19: 1655-1664.

Allinen M, Peri L, Kujala S, Lahti‐Domenici J, Outila K, Karppinen SM, Launonen V and Winqvist R. 2002. Analysis of 11q21–24 loss of heterozygosity candidate target genes in breast cancer: indications of TSLC1 promoter hypermethylation. *Genes Chromosomes Cancer* 34: 384-389.

Amberger JS, Bocchini CA, Schiettecatte F, Scott AF and Hamosh A. 2015. OMIM. org: Online Mendelian Inheritance in Man (OMIM®), an online catalog of human genes and genetic disorders. *Nucleic Acids Res* 43: D789-D798.

Andolfatto P. 2007. Hitchhiking effects of recurrent beneficial amino acid substitutions in the Drosophila melanogaster genome. *Genome Res* 17: 1755-1762.

Auton A, Brooks LD, Durbin RM, et al. 2015. A global reference for human genetic variation. *Nature* 526: 68-74.

Begun DJ, Holloway AK, Stevens K, et al. 2007. Population genomics: whole-genome analysis of polymorphism and divergence in Drosophila simulans. *PLoS Biol* 5: e310.

Berg JJ and Coop G. 2014. A population genetic signal of polygenic adaptation. *PLoS Genet* 10: e1004412.

Berg JJ and Coop G. 2015. A Coalescent Model for a Sweep of a Unique Standing Variant. *Genetics* 201: 707-725.

Birky CW and Walsh JB. 1988. Effects of linkage on rates of molecular evolution. *Proceedings of the National Academy of Sciences* 85: 6414-6418.

Boyko AR, Williamson SH, Indap AR, et al. 2008. Assessing the evolutionary impact of amino acid mutations in the human genome. *PLoS Genet* 4: e1000083.

Bryk J, Hardouin E, Pugach I, Hughes D, Strotmann R, Stoneking M and Myles S. 2008. Positive selection in East Asians for an EDAR allele that enhances NF-κB activation. *PLoS ONE* 3: e2209.

Charlesworth B, Morgan M and Charlesworth D. 1993. The effect of deleterious mutations on neutral molecular variation. *Genetics* 134: 1289-1303.

Chatr-Aryamontri A, Breitkreutz B-J, Oughtred R, et al. 2015. The BioGRID interaction database: 2015 update. *Nucleic Acids Res* 43: D470-D478.

669 Chun S and Fay JC. 2011. Evidence for hitchhiking of deleterious mutations within the human genome.
670 *PLoS Genet* 7: e1002240.
671 Cotney J, Leng J, Yin J, Reilly SK, DeMare LE, Emera D, Ayoub AE, Rakic P and Noonan JP. 2013. The
672 Evolution of Lineage-Specific Regulatory Activities in the Human Embryonic Limb. *Cell* 154:
673 185-196.
674 Dunham I, Kundaje A, Aldred SF, et al. 2012. An integrated encyclopedia of DNA elements in the human
675 genome. *Nature* 489: 57-74.
676 Enard D, Cai L, Gwennap C and Petrov DA. 2016. Viruses are a dominant driver of protein adaptation in
677 mammals. *eLife* 5: e12469.
678 Enard D, Messer PW and Petrov DA. 2014. Genome-wide signals of positive selection in human
679 evolution. *Genome Res* 24: 885-895.
680 Ewing GB and Jensen JD. 2016. The consequences of not accounting for background selection in
681 demographic inference. *Mol Ecol* 25: 135-141.
682 Fagundes NJ, Ray N, Beaumont M, Neuenschwander S, Salzano FM, Bonatto SL and Excoffier L. 2007.
683 Statistical evaluation of alternative models of human evolution. *Proceedings of the National*
684 *Academy of Sciences* 104: 17614-17619.
685 Fan S, Hansen ME, Lo Y and Tishkoff SA. 2016. Going global by adapting local: A review of recent
686 human adaptation. *Science* 354: 54-59.
687 Faraji F, Pang Y, Walker RC, Borges RN, Yang L and Hunter KW. 2012. Cadm1 is a metastasis
688 susceptibility gene that suppresses metastasis by modifying tumor interaction with the cell-
689 mediated immunity. *PLoS Genet* 8: e1002926.
690 Fay JC and Wu C-I. 2000. Hitchhiking under positive Darwinian selection. *Genetics* 155: 1405-1413.
691 Field Y, Boyle EA, Telis N, et al. 2016. Detection of human adaptation during the past 2000 years.
692 *Science* 354: 760-764.
693 Forbes SA, Beare D, Gunasekaran P, et al. 2015. COSMIC: exploring the world's knowledge of somatic
694 mutations in human cancer. *Nucleic Acids Res* 43: D805-D811.
695 Fu Y-X. 1997. Statistical tests of neutrality of mutations against population growth, hitchhiking and
696 background selection. *Genetics* 147: 915-925.
697 Fujita E, Dai H, Tanabe Y, Zhiling Y, Yamagata T, Miyakawa T, Tanokura M, Momoi M and Momoi T.
698 2010. Autism spectrum disorder is related to endoplasmic reticulum stress induced by mutations
699 in the synaptic cell adhesion molecule, CADM1. *Cell death & disease* 1: e47.
700 Fujita E, Tanabe Y, Imhof BA, Momoi MY and Momoi T. 2012. A complex of synaptic adhesion
701 molecule CADM1, a molecule related to autism spectrum disorder, with MUPP1 in the
702 cerebellum. *J Neurochem* 123: 886-894.
703 Fukuhara H, Kuramochi M, Fukami T, et al. 2002. Promoter methylation of TSLC1 and tumor
704 suppression by its gene product in human prostate cancer. *Jpn J Cancer Res* 93: 605-609.
705 Garud NR, Messer PW, Buzbas EO and Petrov DA. 2015. Recent selective sweeps in North American
706 Drosophila melanogaster show signatures of soft sweeps. *PLoS Genet* 11: e1005004.
707 Gazave E, Ma L, Chang D, et al. 2014. Neutral genomic regions refine models of recent rapid human
708 population growth. *Proceedings of the National Academy of Sciences* 111: 757-762.
709 Geurts P, Ernst D and Wehenkel L. 2006. Extremely randomized trees. *Machine Learning* 63: 3-42.
710 Gillespie JH. 1991. The causes of molecular evolution. Oxford: Oxford University Press.
711 Gillespie JH. 2000. Genetic drift in an infinite population: the pseudohitchhiking model. *Genetics* 155:
712 909-919.

713 Gravel S, Henn BM, Gutenkunst RN, et al. 2011. Demographic history and rare allele sharing among
714 human populations. *Proceedings of the National Academy of Sciences* 108: 11983-11988.
715 Griffith OL, Montgomery SB, Bernier B, et al. 2008. ORegAnno: an open-access community-driven
716 resource for regulatory annotation. *Nucleic Acids Res* 36: D107-D113.
717 Harrow J, Frankish A, Gonzalez JM, et al. 2012. GENCODE: The reference human genome annotation
718 for The ENCODE Project. *Genome Res* 22: 1760-1774.
719 Hartfield M and Otto SP. 2011. Recombination and hitchhiking of deleterious alleles. *Evolution* 65:
720 2421-2434.
721 Helgason A, Pálsson S, Thorleifsson G, et al. 2007. Refining the impact of TCF7L2 gene variants on type
722 2 diabetes and adaptive evolution. *Nat Genet* 39: 218-225.
723 Hermisson J and Pennings PS. 2005. Soft sweeps molecular population genetics of adaptation from
724 standing genetic variation. *Genetics* 169: 2335-2352.
725 Hernandez RD, Kelley JL, Elyashiv E, Melton SC, Auton A, McVean G, Sella G and Przeworski M.
726 2011. Classic selective sweeps were rare in recent human evolution. *Science* 331: 920-924.
727 Huerta-Sánchez E, Jin X, Bianba Z, et al. 2014. Altitude adaptation in Tibetans caused by introgression of
728 Denisovan-like DNA. *Nature* 512: 194-197.
729 Huff CD, Witherspoon DJ, Zhang Y, et al. 2012. Crohn's disease and genetic hitchhiking at IBD5. *Mol*
730 *Biol Evol* 29: 101-111.
731 Innan H and Kim Y. 2004. Pattern of polymorphism after strong artificial selection in a domestication
732 event. *Proc Natl Acad Sci U S A* 101: 10667-10672.
733 Jensen JD, Thornton KR and Andolfatto P. 2008. An approximate Bayesian estimator suggests strong,
734 recurrent selective sweeps in Drosophila. *PLoS Genet* 4: e1000198.
735 Jones DA and Wakeley J. 2008. The influence of gene conversion on linkage disequilibrium around a
736 selective sweep. *Genetics* 180: 1251-1259.
737 Kanehisa M, Sato Y, Kawashima M, Furumichi M and Tanabe M. 2015. KEGG as a reference resource
738 for gene and protein annotation. *Nucleic Acids Res*: gkv1070.
739 Kaplan NL, Hudson R and Langley C. 1989. The" hitchhiking effect" revisited. *Genetics* 123: 887-899.
740 Karasov T, Messer PW and Petrov DA. 2010. Evidence that adaptation in Drosophila is not limited by
741 mutation at single sites. *PLoS Genet* 6: e1000924.
742 Karolchik D, Hinrichs AS, Furey TS, Roskin KM, Sugnet CW, Haussler D and Kent WJ. 2004. The
743 UCSC Table Browser data retrieval tool. *Nucleic Acids Res* 32: D493-D496.
744 Kelly JK. 1997. A test of neutrality based on interlocus associations. *Genetics* 146: 1197-1206.
745 Kent WJ. 2002. BLAT—the BLAST-like alignment tool. *Genome Res* 12: 656-664.
746 Kent WJ, Sugnet CW, Furey TS, Roskin KM, Pringle TH, Zahler AM and Haussler D. 2002. The human
747 genome browser at UCSC. *Genome Res* 12: 996-1006.
748 Kern AD, Jones CD and Begun DJ. 2002. Genomic effects of nucleotide substitutions in Drosophila
749 simulans. *Genetics* 162: 1753-1761.
750 Kern AD and Schrider DR. 2016. discoal: flexible coalescent simulations with selection. *Bioinformatics*:
751 btw556.
752 Kim Y and Nielsen R. 2004. Linkage disequilibrium as a signature of selective sweeps. *Genetics* 167:
753 1513-1524.
754 Kim Y and Stephan W. 2002. Detecting a local signature of genetic hitchhiking along a recombining
755 chromosome. *Genetics* 160: 765-777.

Kohda K, Kamiya Y, Matsuda S, Kato K, Umemori H and Yuzaki M. 2003. Heteromer formation of δ2 glutamate receptors with AMPA or kainate receptors. *Molecular Brain Research* 110: 27-37.

Kong A, Frigge ML, Masson G, et al. 2012. Rate of *de novo* mutations and the importance of father's age to disease risk. *Nature* 488: 471-475.

Kong A, Thorleifsson G, Gudbjartsson DF, et al. 2010. Fine-scale recombination rate differences between sexes, populations and individuals. *Nature* 467: 1099-1103.

Kumar P, Henikoff S and Ng PC. 2009. Predicting the effects of coding non-synonymous variants on protein function using the SIFT algorithm. *Nat Protoc* 4: 1073-1081.

Kuramochi M, Fukuhara H, Nobukuni T, et al. 2001. TSLC1 is a tumor-suppressor gene in human non-small-cell lung cancer. *Nat Genet* 27: 427-430.

Lander ES, Linton LM, Birren B, et al. 2001. Initial sequencing and analysis of the human genome. *Nature* 409: 860-921.

Landrum MJ, Lee JM, Benson M, et al. 2016. ClinVar: public archive of interpretations of clinically relevant variants. *Nucleic Acids Res* 44: D862-D868.

Langley CH, Stevens K, Cardeno C, et al. 2012. Genomic variation in natural populations of *Drosophila melanogaster*. *Genetics* 192: 533-598.

Lee YCG, Langley CH and Begun DJ. 2013. Differential strengths of positive selection revealed by hitchhiking effects at small physical scales in Drosophila melanogaster. *Mol Biol Evol*: mst270.

Li H. 2011. A new test for detecting recent positive selection that is free from the confounding impacts of demography. *Mol Biol Evol* 28: 365-375.

Li H and Durbin R. 2011. Inference of human population history from individual whole-genome sequences. *Nature* 475: 493-496.

Li MJ, Wang LY, Xia Z, Wong MP, Sham PC and Wang J. 2013. dbPSHP: a database of recent positive selection across human populations. *Nucleic Acids Res*: gkt1052.

Lin K, Li H, Schlötterer C and Futschik A. 2011. Distinguishing positive selection from neutral evolution: boosting the performance of summary statistics. *Genetics* 187: 229-244.

Liu X, Somel M, Tang L, et al. 2012. Extension of cortical synaptic development distinguishes humans from chimpanzees and macaques. *Genome Res* 22: 611-622.

Liu X, Wu C, Li C and Boerwinkle E. 2016. dbNSFP v3. 0: A One‐Stop Database of Functional Predictions and Annotations for Human Nonsynonymous and Splice‐Site SNVs. *Hum Mutat* 37: 235-241.

Lohmueller KE, Albrechtsen A, Li Y, et al. 2011. Natural selection affects multiple aspects of genetic variation at putatively neutral sites across the human genome. *PLoS Genet* 7: e1002326.

Lonsdale J, Thomas J, Salvatore M, et al. 2013. The genotype-tissue expression (GTEx) project. *Nat Genet* 45: 580-585.

Luján R, Shigemoto R and Lopez-Bendito G. 2005. Glutamate and GABA receptor signalling in the developing brain. *Neuroscience* 130: 567-580.

Macpherson JM, Sella G, Davis JC and Petrov DA. 2007. Genomewide spatial correspondence between nonsynonymous divergence and neutral polymorphism reveals extensive adaptation in Drosophila. *Genetics* 177: 2083-2099.

Marsden CD, Ortega-Del Vecchyo D, O'Brien DP, et al. 2016. Bottlenecks and selective sweeps during domestication have increased deleterious genetic variation in dogs. *Proceedings of the National Academy of Sciences* 113: 152-157.

799 Marth GT, Czabarka E, Murvai J and Sherry ST. 2004. The allele frequency spectrum in genome-wide
800 human variation data reveals signals of differential demographic history in three large world
801 populations. *Genetics* 166: 351-372.
802 Maynard Smith J and Haigh J. 1974. The hitch-hiking effect of a favourable gene. *Genet Res* 23: 23-35.
803 Meyer KA, Marques-Bonet T and Sestan N. 2017. Differential Gene Expression in the Human Brain Is
804 Associated with Conserved, but not Accelerated, Noncoding Sequences. *Mol Biol Evol* 34: 1217-
805 1229.
806 Nei M and Li W-H. 1979. Mathematical model for studying genetic variation in terms of restriction
807 endonucleases. *Proceedings of the National Academy of Sciences* 76: 5269-5273.
808 Nielsen R, Bustamante C, Clark AG, et al. 2005a. A scan for positively selected genes in the genomes of
809 humans and chimpanzees. *PLoS Biol* 3: e170.
810 Nielsen R, Williamson S, Kim Y, Hubisz MJ, Clark AG and Bustamante C. 2005b. Genomic scans for
811 selective sweeps using SNP data. *Genome Res* 15: 1566-1575.
812 Nunney L and Muir B. 2015. Peto's paradox and the hallmarks of cancer: constructing an evolutionary
813 framework for understanding the incidence of cancer. *Phil Trans R Soc B* 370: 20150161.
814 Orr HA and Betancourt AJ. 2001. Haldane's sieve and adaptation from the standing genetic variation.
815 *Genetics* 157: 875-884.
816 Orr HA and Unckless RL. 2014. The population genetics of evolutionary rescue. *PLoS Genet* 10:
817 e1004551.
818 Pavlidis P, Jensen JD and Stephan W. 2010. Searching for footprints of positive selection in whole-
819 genome SNP data from nonequilibrium populations. *Genetics* 185: 907-922.
820 Pei B, Sisu C, Frankish A, et al. 2012. The GENCODE pseudogene resource. *Genome Biol* 13: 1.
821 Pennings PS and Hermisson J. 2006a. Soft sweeps II—molecular population genetics of adaptation from
822 recurrent mutation or migration. *Mol Biol Evol* 23: 1076-1084.
823 Pennings PS and Hermisson J. 2006b. Soft sweeps III: the signature of positive selection from recurrent
824 mutation. *PLoS Genet* 2: e186.
825 Peter BM, Huerta-Sanchez E and Nielsen R. 2012. Distinguishing between selective sweeps from
826 standing variation and from a *de novo* mutation. *PLoS Genet* 8: e1003011.
827 Pickrell JK, Coop G, Novembre J, et al. 2009. Signals of recent positive selection in a worldwide sample
828 of human populations. *Genome Res* 19: 826-837.
829 Przeworski M, Coop G and Wall JD. 2005. The signature of positive selection on standing genetic
830 variation. *Evolution* 59: 2312-2323.
831 Pybus M, Dall'Olio GM, Luisi P, Uzkudun M, Carreño-Torres A, Pavlidis P, Laayouni H, Bertranpetit J
832 and Engelken J. 2013. 1000 Genomes Selection Browser 1.0: a genome browser dedicated to
833 signatures of natural selection in modern humans. *Nucleic Acids Res*: gkt1188.
834 Pybus M, Luisi P, Dall'Olio GM, Uzkudun M, Laayouni H, Bertranpetit J and Engelken J. 2015.
835 Hierarchical boosting: a machine-learning framework to detect and classify hard selective sweeps
836 in human populations. *Bioinformatics*: btv493.
837 Qian W, Zhou H and Tang K. 2015. Recent Coselection in Human Populations Revealed by Protein–
838 Protein Interaction Network. *Genome Biol Evol* 7: 136-153.
839 Ronen R, Udpa N, Halperin E and Bafna V. 2013. Learning natural selection from the site frequency
840 spectrum. *Genetics* 195: 181-193.
841 Ruwende C, Khoo S, Snow R, et al. 1995. Natural selection of hemi-and heterozygotes for G6PD
842 deficiency in Africa by resistance to severe malaria. *Nature* 376: 246-249.

Sabeti PC, Reich DE, Higgins JM, et al. 2002. Detecting recent positive selection in the human genome from haplotype structure. *Nature* 419: 832-837.

Sabeti PC, Varilly P, Fry B, et al. 2007. Genome-wide detection and characterization of positive selection in human populations. *Nature* 449: 913-918.

Sattath S, Elyashiv E, Kolodny O, Rinott Y and Sella G. 2011. Pervasive adaptive protein evolution apparent in diversity patterns around amino acid substitutions in Drosophila simulans. *PLoS Genet* 7: e1001302.

Schrider DR and Kern AD. 2015. Inferring selective constraint from population genomic data suggests recent regulatory turnover in the human brain. *Genome Biol Evol* 7: 3511-3528.

Schrider DR and Kern AD. 2016. S/HIC: Robust Identification of Soft and Hard Sweeps Using Machine Learning. *PLoS Genet* 12: e1005928.

Schrider DR, Mendes FK, Hahn MW and Kern AD. 2015. Soft shoulders ahead: spurious signatures of soft and partial selective sweeps result from linked hard sweeps. *Genetics* 200: 267-284.

Schrider DR, Shanku AG and Kern AD. 2016. Effects of Linked Selective Sweeps on Demographic Inference and Model Selection. *Genetics* 204: 1207-1223.

Sheehan S and Song YS. 2016. Deep learning for population genetic inference. *PLoS Comput Biol* 12: e1004845.

Siepel A, Bejerano G, Pedersen JS, et al. 2005. Evolutionarily conserved elements in vertebrate, insect, worm, and yeast genomes. *Genome Res* 15: 1034-1050.

Stephan W, Wiehe TH and Lenz MW. 1992. The effect of strongly selected substitutions on neutral polymorphism: analytical results based on diffusion theory. *Theor Popul Biol* 41: 237-254.

Stephens JC, Reich DE, Goldstein DB, et al. 1998. Dating the origin of the CCR5-Δ32 AIDS-resistance allele by the coalescence of haplotypes. *The American Journal of Human Genetics* 62: 1507-1515.

Storey JD. 2002. A direct approach to false discovery rates. *Journal of the Royal Statistical Society: Series B (Statistical Methodology)* 64: 479-498.

Swanson WJ and Vacquier VD. 2002. The rapid evolution of reproductive proteins. *Nature Reviews Genetics* 3: 137-144.

Tajima F. 1989. Statistical method for testing the neutral mutation hypothesis by DNA polymorphism. *Genetics* 123: 585-595.

Thornton KR. 2014. A C++ template library for efficient forward-time population genetic simulation of large populations. *Genetics* 198: 157-166.

Tishkoff SA, Reed FA, Ranciaro A, et al. 2007. Convergent adaptation of human lactase persistence in Africa and Europe. *Nat Genet* 39: 31-40.

UK10K Consortium. 2015. The UK10K project identifies rare variants in health and disease. *Nature* 526: 82-90.

Van Der Weyden L, Arends MJ, Chausiaux OE, et al. 2006. Loss of TSLC1 causes male infertility due to a defect at the spermatid stage of spermatogenesis. *Mol Cell Biol* 26: 3595-3609.

Voight BF, Kudaravalli S, Wen X and Pritchard JK. 2006. A map of recent positive selection in the human genome. *PLoS Biol* 4: e72.

Watterson G. 1975. On the number of segregating sites in genetical models without recombination. *Theor Popul Biol* 7: 256-276.

Welter D, MacArthur J, Morales J, et al. 2014. The NHGRI GWAS Catalog, a curated resource of SNP-trait associations. *Nucleic Acids Res* 42: D1001-D1006.

887 Wiehe T and Stephan W. 1993. Analysis of a genetic hitchhiking model, and its application to DNA
888 polymorphism data from Drosophila melanogaster. *Mol Biol Evol* 10: 842-854.
889 Williamson SH, Hubisz MJ, Clark AG, Payseur BA, Bustamante CD and Nielsen R. 2007. Localizing
890 recent adaptive evolution in the human genome. *PLoS Genet* 3: e90.
891 Wilson BA, Petrov DA and Messer PW. 2014. Soft selective sweeps in complex demographic scenarios.
892 *Genetics* 198: 669-684.
893 Wu YY, Yang Y, Xu YD and Yu HL. 2015. Targeted disruption of the spermatid-specific gene Spata31
894 causes male infertility. *Mol Reprod Dev* 82: 432-440.
895 Yates A, Akanni W, Amode MR, et al. 2016. Ensembl 2016. *Nucleic Acids Res* 44: D710-D716.
896 Zhang P, Si X, Skogerbø G, et al. 2014. piRBase: a web resource assisting piRNA functional study.
897 *Database* 2014: bau110.
898 Zhiling Y, Fujita E, Tanabe Y, Yamagata T, Momoi T and Momoi MY. 2008. Mutations in the gene
899 encoding CADM1 are associated with autism spectrum disorder. *Biochem Biophys Res Commun*
900 377: 926-929.
901
902
903
904
905
906
907
908
909 **Table 1: Number of sweeps of each type detected in each population sample.**
910

Population	# of Hard Sweeps	# of Soft Sweeps	Total # of Sweeps
JPT (Tokyo, Japan)	61 (5.8%)	998 (94.2%)	1,059
CEU (Utah, United States)	66 (6.5%)	947 (93.5%)	1,013
PEL (Lima, Peru)	32 (4.7%)	655 (95.3%)	687
GWD (Western Divisions, the Gambia)	5 (0.6%)	795 (99.4%)	800
YRI (Ibadan, Nigeria)	13 (1.6%)	797 (98.4%)	810
LWK (Webuye, Kenya)	3 (0.4%)	805 (99.6%)	808

911
912

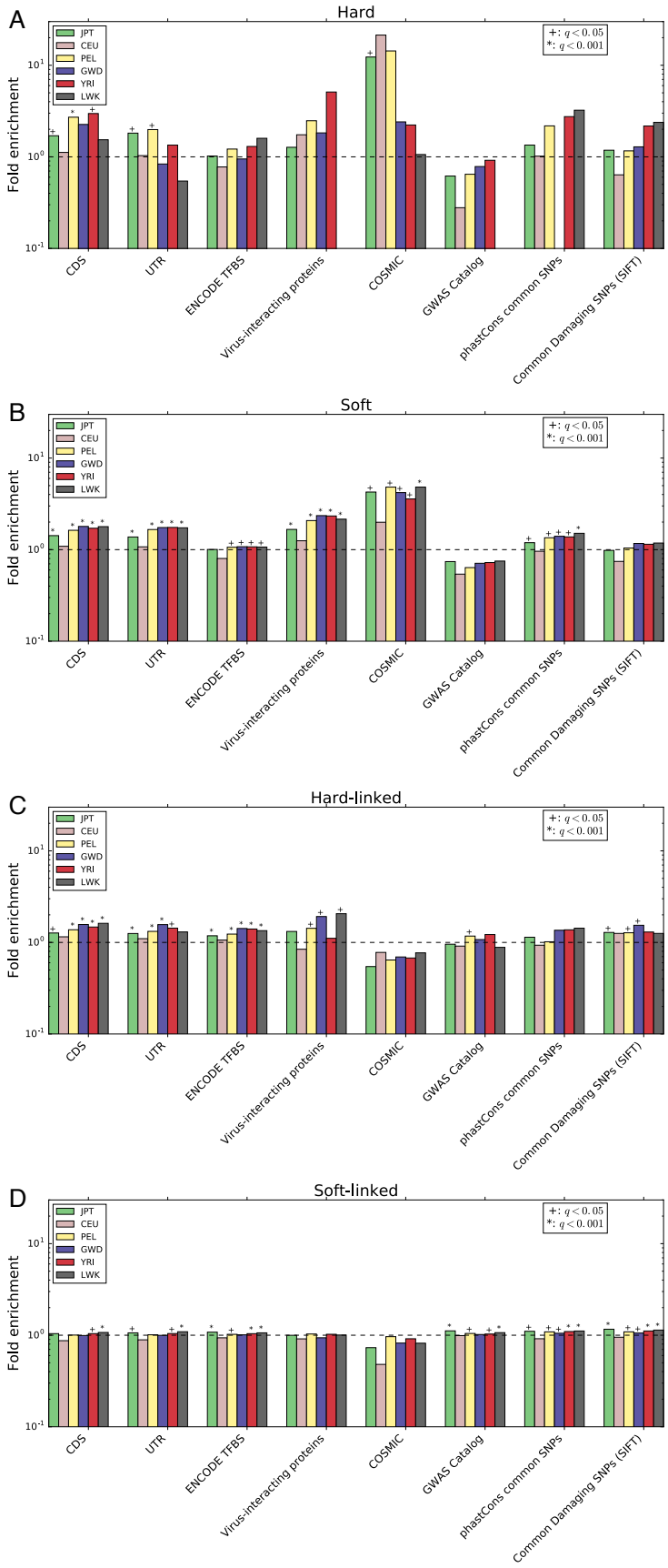

Figure 1: Enrichment of various annotation features in regions classified as sweeps or linked to sweeps relative. The fold enrichment is the ratio of the number of base pairs in the intersection between windows assigned to a given class and an annotation feature divided by the mean of this intersection across the permuted data sets (Methods). This was calculated separately for each population. (A) Enrichment of elements in windows classified as hard sweeps. (B) Same as A, but for soft sweeps. (C) Enrichment of elements in windows classified as affected by linked hard sweeps. (D) Linked soft sweeps.

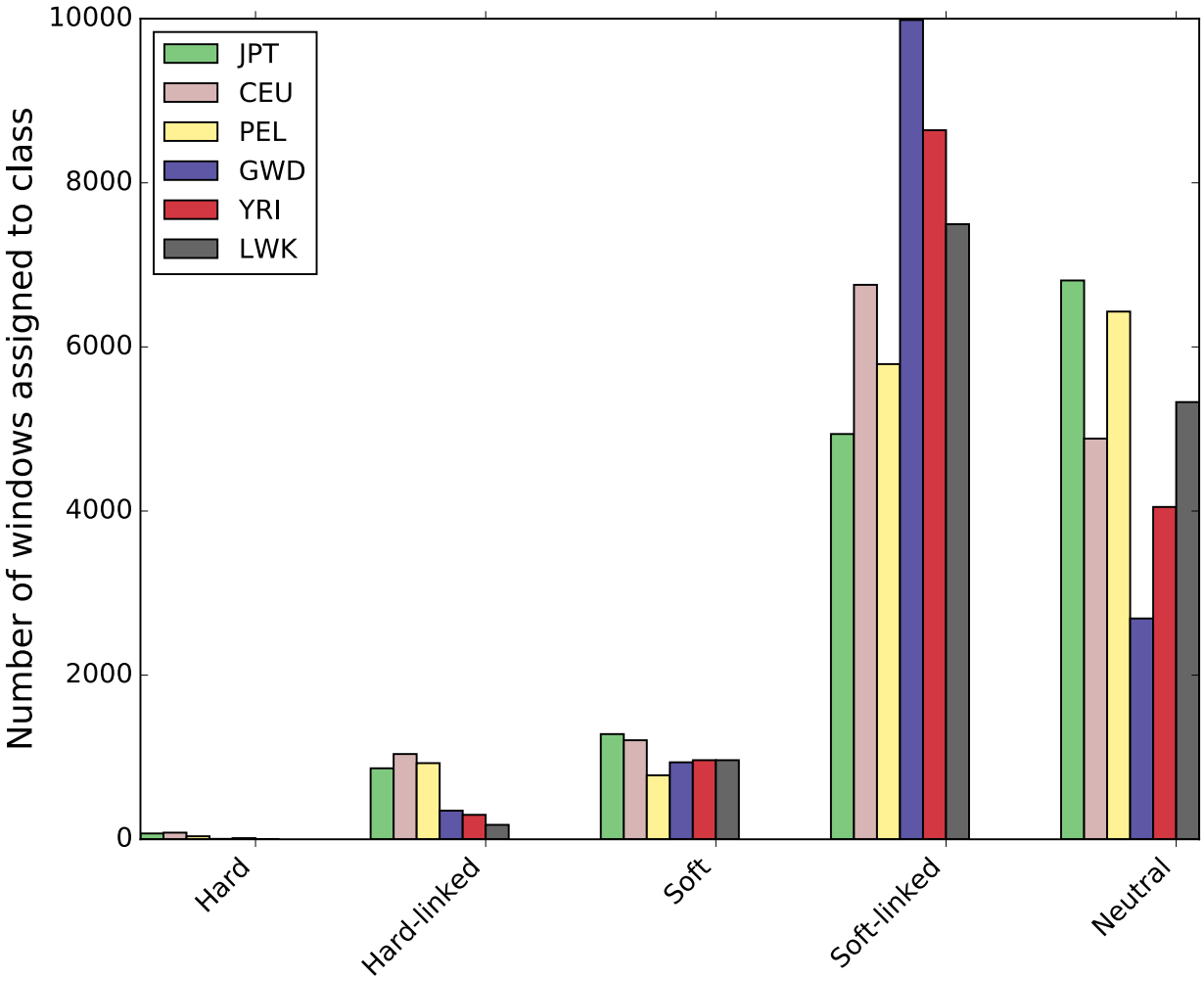

Figure 2: The number of windows assigned to each class by S/HIC in each population.

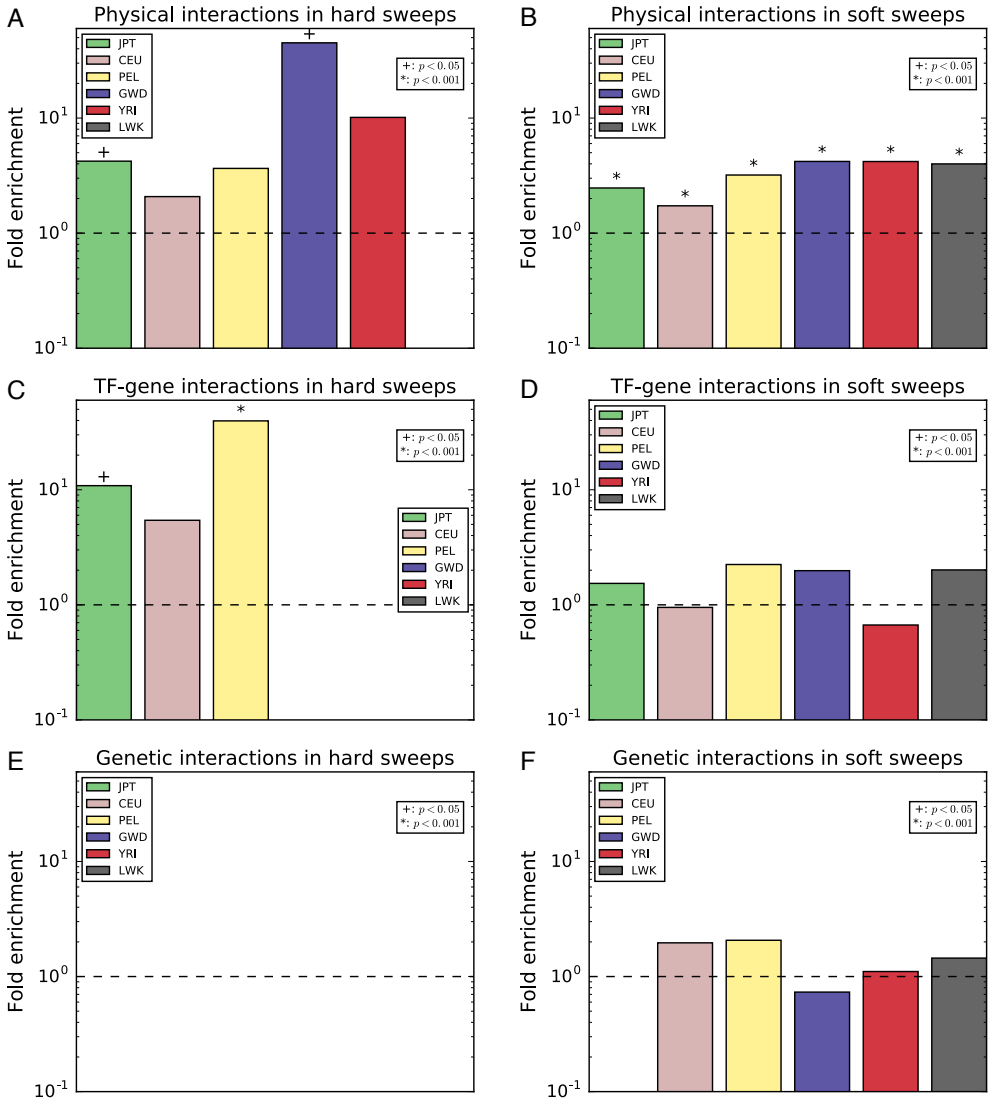

Figure 3: Enrichment of pairs of interacting genes each falling within a window classified as a sweep. The fold enrichment is the ratio of the number of pairs of interacting genes overlapping a window classified as a sweep of a given type divided by the mean of this number across the permuted data sets (Methods). This was calculated separately for each population. When no pairs of interacting sweep genes were observed in our true data set or a population, no bar was drawn. (A) Enrichment of pairs of genes encoding protein products that physically interact with each other (data from BioGRID) and both overlap hard sweep windows. (B) Same as A, but for soft sweeps. (C) Enrichment of pairs of genes, one of which is encodes a transcription factor that affects expression of the other (data from ORegAnno), where both overlap hard sweep windows. (D) Same as D, but for soft sweeps. (E) Enrichment of pairs of genes for which a genetic interaction has been observed (data from BioGRID) and both overlap hard sweep windows. (F) Same as E, but for soft sweeps.

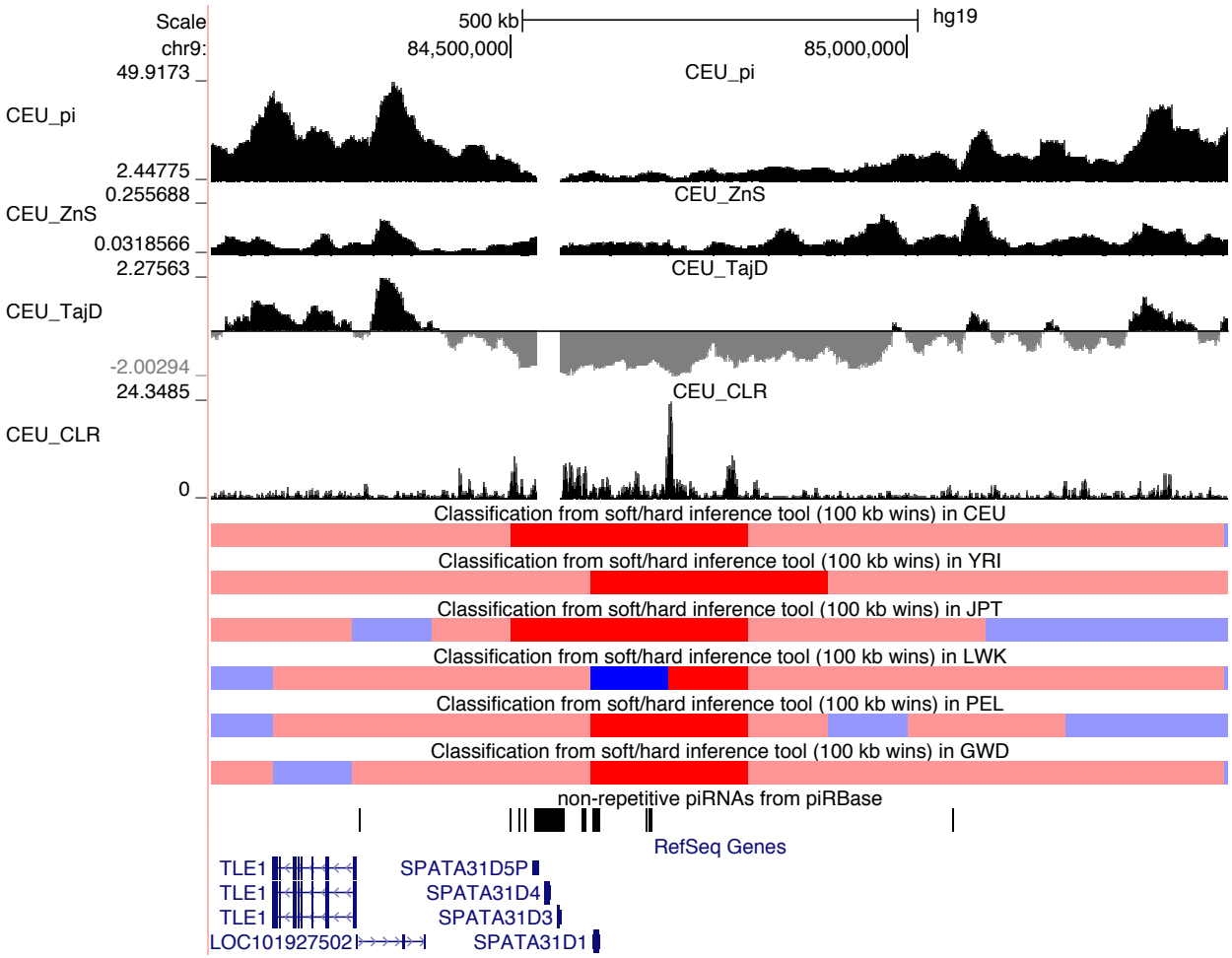

Figure 4: Hard selective sweep near several *SPATA31* spermatogenesis-associated genes. The S/HIC classification tracks show the raw classifier output for each population (red=hard sweep, blue=soft sweep, light red=hard-linked, light blue=soft-linked, black=neutral). We also show the values of various population genetic summary and test statistics (π, Tajima's D, Kelly's Z_{nS}, and the SweepFinder composite likelihood ratio, or CLR). To avoid clutter, we only show statistics from CEU.

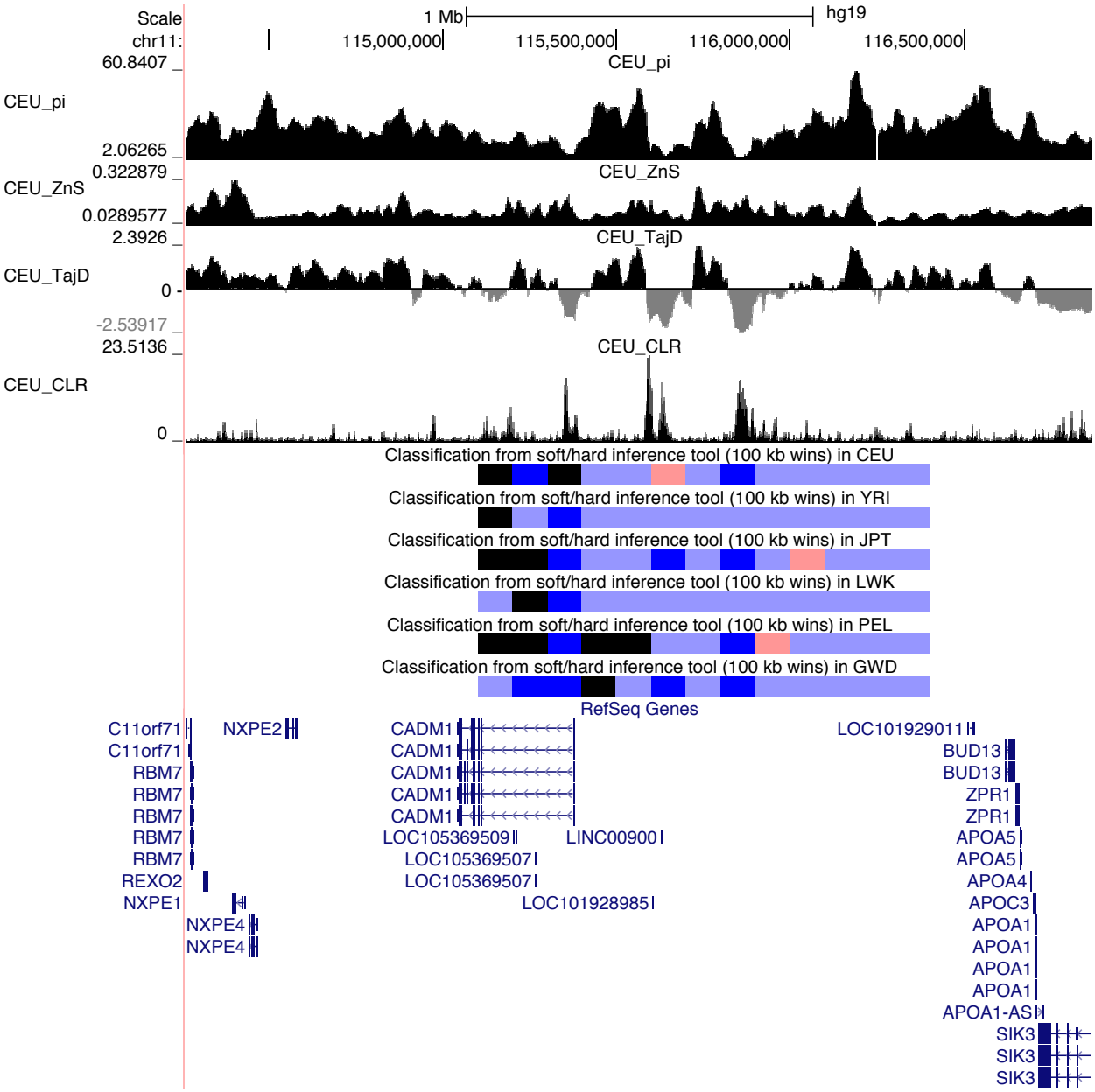

Figure 5: Soft selective sweeps near *CADM1*. The same tracks are shown as in Figure 4.

SUPPLEMENTARY FIGURE AND TABLE LEGENDS

supplementary fig. S1: Heatmaps showing the accuracy of our six classifiers on test data, one for each population. On the *y*-axis, we show the location of the sweep relative to the classified window (i.e. the central sub-window), with the exception of the "Neutral" case where there is no sweep. The test data were simulated under the same demographic models used for training. On the *x*-axis we show the class inferred by S/HIC. A perfect classifier would infer "Hard" for 100% test instance where a hard sweep is in the focal sub-window (and analogously for soft sweeps), "Hard-linked" for 100% of cases where a hard sweep occurs elsewhere (and analogously for soft sweeps not located in the central sub-window), and "Neutral" for 100% of cases with no sweep. Both GWD and JPT also contain test results on a simulated set of examples of purifying/background selection. (A) Test results for CEU. (B) GWD. (C) JPT. (D) LWK. (E) PEL. (F) YRI.

supplementary fig. S2: Histograms of H_{12} and H_2/H_1 within windows classified has hard sweeps, soft sweeps, or neutral for each population.

supplementary fig. S3: Soft selective sweep in *GRIA2*. The same tracks are shown as in figs. 4 and 5.

supplementary fig. S4: False positive and false negative rates on simulated test data with varying values of θ. For each population, we used discoal to simulate 100 replicates for each combination of S/HIC's five classes and three fixed values of θ. In these simulations all parameters other than θ had the same values as in supplementary table S5. "Medium" θ refers to the mean value of θ used for a given population's training and testing simulations (Methods), while "Low" and "High" θ refer to one-half and double this value, respectively. Examples of the Hard-linked, Soft-linked, or Neutral classes that are classified as sweeps represent false positives, while Hard and Soft examples not classified as sweeps are false negatives.

supplementary table S1: Number of sweeps found in each subset of populations.

supplementary table S2: Numbers of hard and soft sweeps found in each population when imposing various posterior probability thresholds to S/HIC's classifications.

supplementary table S3: Enrichment of various sequence annotations in each S/HIC class.

supplementary table S4: Enrichment of annotation terms in hard and soft sweeps (only terms with q<0.05 for at least one sweep type in at least one population are shown).

supplementary table S5: Example command lines used to generate training data for each population, with a soft sweep occurring in the central sub-window.